Astron. Astrophys. 345, 363–368 (1999)

ASTRONOMY AND ASTROPHYSICS

ESO imaging survey

V. Cluster search using color data

L.F. Olsen[1,2], M. Scodeggio[1], L. da Costa[1], R. Slijkhuis[1,3], C. Benoist[1,4], E. Bertin[1,3,5], E. Deul[1,3], T. Erben[1,6], M.D. Guarnieri[1,7], R. Hook[8], M. Nonino[1,9], I. Prandoni[1,10], A. Wicenec[1], and S. Zaggia[1,11]

[1] European Southern Observatory, Karl-Schwarzschild-Strasse 2, D-85748 Garching bei München, Germany
[2] Astronomisk Observatorium, Juliane Maries Vej 30, DK-2100 Copenhagen, Denmark
[3] Leiden Observatory, P.O. Box 9513, 2300 RA Leiden, The Netherlands
[4] DAEC, Observatoire de Paris-Meudon, 5 Pl. J. Janssen, F-92195 Meudon Cedex, France
[5] Institut d'Astrophysique de Paris, 98bis Bd Arago, F-75014 Paris, France
[6] Max-Planck-Institut für Astrophysik, Postfach 1523, D-85748 Garching bei München, Germany
[7] Osservatorio Astronomico di Pino Torinese, Strada Osservatorio 20, I-10025 Torino, Italy
[8] Space Telescope – European Coordinating Facility, Karl-Schwarzschild-Strasse 2, D-85748 Garching bei München, Germany
[9] Osservatorio Astronomico di Trieste, Via G.B. Tiepolo 11, I-31144 Trieste, Italy
[10] Istituto di Radioastronomia del CNR, Via Gobetti 101, I-40129 Bologna, Italy
[11] Osservatorio Astronomico di Capodimonte, Via Moiariello 15, I-80131 Napoli, Italy

Received 16 December 1998 / Accepted 1 March 1999

Abstract. This paper presents 19 candidate clusters detected using the galaxy catalog extracted from the I-band images taken for the ESO Imaging Survey (EIS). The candidates are found over a region of 1.1 square degrees, located near the South Galactic Pole (EIS Patch B). Combined with the sample reported earlier, the number of candidates in the Southern Galactic Cap is now 54 over a total area of ~ 3.6 square degrees. V-band images are also available over 2.9 square degrees, and galaxy catalogs extracted from them over a uniform area of 2 square degrees have been used to further explore the reality of the cluster candidates detected in I-band. Nearly all the candidates detected in I-band with estimated redshifts $z \leq 0.5$ are also identified in V. At higher redshifts, only rich candidates are detected in both bands.

Key words: galaxies: clusters: general – cosmology: large-scale structure of Universe – cosmology: observations

1. Introduction

The ESO Imaging Survey (EIS; Renzini & da Costa 1997) is the outgrowth of a concerted effort between ESO and its community to carry out an imaging survey and provide candidate targets for the rapidly approaching first year of regular operation of the VLT. The main science goals of the survey have been described earlier (Nonino et al. 1998, Paper I, Prandoni et al. 1998, Paper III). These papers also include a detailed account of the survey observing strategy, and of the data obtained for two of the four areas covered by the survey (EIS patches A and B, at $\alpha \approx 22^h40^m$, $\delta \approx -40^\circ$ and $\alpha \approx 00^h50^m$, $\delta \approx -29^\circ30'$, respectively). One of the main goals of EIS is the compilation of a list of candidate clusters of galaxies, spanning a large redshift range. Following the timetable recommended by the EIS Working Group, lists of cluster candidates in the various areas covered by the survey are being prepared and made public as soon as they become available. In addition, an interface with the ESO Science Archive has been created, allowing image postage stamps of the candidates to be extracted for visual inspection and preparation of finding charts (see "http://www.eso.org/eis").

A preliminary catalog containing 35 cluster candidates identified in EIS patch A, was presented in a previous paper (Olsen et al. 1998, hereafter Paper II). As emphasized in that paper, the goal of the EIS cluster search has been to prepare a list of *candidates* for follow-up observations and not to produce a well-defined sample for statistical analysis. For the cluster search the matched filter algorithm discussed by Postman et al. (1996) was chosen, since it has already been tested and used to analyze similar data. Moreover, by using the same algorithm the results obtained here can be easily compared to those obtained by those authors. Since the data are public, other groups may produce their own catalogs using different methods. A comparison of various catalogs will be instructive in evaluating the strengths and weaknesses of different algorithms.

While completeness is an important issue for statistical studies, the main concern of the EIS cluster search program is the reliability of the candidates, and therefore the minimization of the number of false detections, to optimize any future follow-up work. To minimize contamination by spurious detections, the analysis has been restricted to the most uniform surveyed areas. Moreover, the parameters adopted in searching for candidates have been conservatively chosen, based on the results of an ex-

Send offprint requests to: L.F. Olsen

tensive set of simulations, to minimize the contamination by noise peaks (Paper II).

Another way of further testing the reality of the detections is to use data in different passbands. In Paper II candidate clusters were detected using only I-band data. Currently, however, V-band galaxy catalogs are available for ~ 2.9 square degrees. The availability of these data allows one to detect clusters in the V-band and cross-identify them with those detected in the I-band. The color information can be used: 1) to confirm the reality of detections directly from the cross-identification; 2) to confirm detections by identifying the expected sequence of cluster early-type galaxies in the color-magnitude (CM) diagram; 3) to use the CM relation to independently check the estimated cluster redshift and select targets for follow-up spectroscopy.

The goals of the present paper are to add to the list of EIS I-band cluster candidates those detected in patch B and to investigate what additional information the V-band data provide over the region where V and I images overlap. The data are described in Sect. 2; Sect. 3 describes the cluster candidate catalog and the investigation of the color information; the conclusions are summarized in Sect. 4.

2. The data

Although the original intention of EIS was to cover the entire survey area in V and I, this proved impossible due to the bad weather conditions in the period July–December 1997. As a consequence, the observations in the V-band were discontinued after the completion of patch B, to enlarge as much as possible the area covered in I-band. Nevertheless, available V-band images overlap I-band observations over an area of 1.2 and 1.7 square degrees in patches A and B, respectively. Due to varying observing conditions the quality of the data is not uniform over the entire overlap region. This can be seen from the seeing and limiting isophote distributions shown in Papers I and III. This information was used to eliminate regions with significantly shallower limiting magnitudes, due to poor transparency, and the following analysis is restricted to areas of $\simeq 0.9$ (patch A) and $\simeq 1.1$ (patch B) square degrees. The median seeing value for all the observations in the area being analyzed is $\simeq 1$ arcsec.

The data were reduced using the EIS reduction pipeline which routinely produces single-frame catalogs, that are associated to produce the so-called even and odd catalogs (see Papers I and II). This procedure has been performed independently for the V and I images, yielding two independent catalogs for each band and each patch. The limiting magnitude for star-galaxy separation in the I-band was established in Papers I and II to be $I \sim 21$. Brighter than this magnitude only objects with stellarity index less than 0.75 were taken to be galaxies, while all fainter objects were included in the galaxy catalogs. For the V-band the limit for star-galaxy separation was found to be $V \sim 22$ and galaxies were selected following the same procedure. As shown in Papers I and III the 80% completeness limits of the galaxy catalogs extracted from single exposures are typically $V \sim 24.0$ and $I \sim 23.0$.

3. Results

3.1. Detected cluster candidates

Using the various odd/even catalogs containing the objects extracted from single frames (150 sec exposures), lists of cluster candidates have been produced for each patch and band using the cluster identification pipeline based on the matched-filter method described in detail in Paper II. The cluster identification has been applied to the I-band data from patch B, using the same parameters to describe the cluster radial profile and luminosity function ($r_c = 100h^{-1}$kpc, $r_{co} = 1h^{-1}$Mpc and $M_I^* = -22.33$, $\alpha = -1.1$), the same SExtractor detection parameters ($\sigma_{det} = 2.0$ and N_{min} corresponding to the area of a circle with radius $1r_c$), and the same selection criteria ($n_z \geq 4$, $\sigma \geq 3$ and $\Lambda_{cl} \geq 30$) as given in Paper II. Over the analyzed area of 1.1 square degrees, 19 new cluster candidates were found, which gives a density of 17.2 cluster candidates per square degree, consistent with the results discussed in Paper II and with the value estimated by Postman et al. (1996). Out of the 19 detections 12 are "good" candidates, *i.e.*, those detected at 4σ in at least one catalog, or at 3σ in both I-band catalogs. In addition, there are 7 candidates detected at 3σ in only one catalog, nearly all at large redshift ($z \gtrsim 0.6$). In Paper II the noise properties of the cluster-finding procedure were investigated and the frequency of 3σ noise peaks was estimated to be 4.2 per square degree. Using this noise frequency it is found that the number of questionable candidates is consistent with that expected for noise peaks, about 5 in the area analyzed in Patch B.

The properties of the detected cluster candidates are summarized in Table 1 which gives: in Column (1) the cluster id; in Columns (2) and (3) the right ascension and declination (J2000); in Column (4) the estimated redshift; in Column (5) the measure of the cluster richness derived from the maximum likelihood (see Paper II, Eq. (1)); Column (6) gives the number of galaxies within a magnitude interval of 2 magnitudes delimited at the bright end by the magnitude of third brightest cluster galaxy; in Columns (7) and (8) the significance of the detections in the even and odd catalogs, respectively; in Column (9) the significance of the detection using the galaxy catalogs extracted from the V images (see below); and in Column (10) other identifications. The upper part of the table lists the "good" candidates, while the remaining candidates are listed in the lower part of the table. Note that the detection with the largest significance is the cluster easily seen near the center of the patch. This cluster is Abell S84 at $z \sim 0.1$ (Abell et al. 1989, Strubble & Rood 1987).

For simultaneous display of the cluster candidates in all available passbands a new facility for extracting image postage stamps from the coadded images was implemented in the ESO Science Archive. Using this facility all cluster candidates detected in I-band were visually inspected and most were found to be promising. Even though candidates in the lower part of the table are less conspicuous, most do seem to be possible clusters. Out of the seven candidates listed in the bottom part of the table, at least 4 lie in a region where the limiting isophote varies significantly between the odd and even frames which may ex-

Table 1. Preliminary cluster candidates for EIS Patch B.

Cluster name	α (J2000)	δ (J2000)	z	Λ_{cl}	N_R	σ_{even}	σ_{odd}	σ_V	Notes
EIS 0044−2950	00 44 58.6	−29 50 49.5	0.3	23.1	20	3.2	3.6	3.6	
EIS 0045−2923	00 45 14.4	−29 23 43.4	0.2	33.8	100	7.1	7.1	7.7	
EIS 0046−2925	00 46 07.4	−29 25 42.2	0.2	44.4	26	–	6.9	4.2	
EIS 0046−2951	00 46 07.4	−29 51 44.5	0.9	157.0	2	3.1	3.2	–	
EIS 0048−2928	00 48 25.8	−29 28 50.1	0.4	36.6	31	3.5	3.6	6.0	
EIS 0048−2942	00 48 31.6	−29 42 25.1	0.6	55.6	13	4.3	4.1	2.7	
EIS 0049−2931	00 49 23.1	−29 31 56.8	0.2	84.2	48	14.6	14.8	18.4	S84
EIS 0049−2920	00 49 31.3	−29 20 34.1	0.3	35.7	13	4.3	4.0	3.5	
EIS 0050−2941	00 50 04.4	−29 41 35.6	1.0	175.3	62	3.4	3.9	3.5	
EIS 0052−2927	00 52 49.5	−29 27 57.2	0.9	121.5	34	3.5	3.6	–	
EIS 0052−2923	00 52 59.6	−29 23 14.1	0.2	26.7	14	5.0	–	5.8	
EIS 0044−2950	00 44 36.5	−29 50 12.2	0.9	128.1	35	–	3.6	–	
EIS 0045−2944	00 45 00.8	−29 44 57.7	0.4	35.5	24	–	3.3	3.2	
EIS 0045−2951	00 45 14.9	−29 51 58.6	0.8	86.5	15	–	3.6	–	
EIS 0045−2948	00 45 44.4	−29 48 27.1	0.5	39.6	29	2.9	3.2	2.6	
EIS 0045−2929	00 45 51.3	−29 29 38.7	1.1	236.8	6	–	3.1	3.3	
EIS 0046−2945	00 46 19.5	−29 45 47.1	1.0	285.6	82	3.6	–	–	
EIS 0046−2930	00 46 29.6	−29 30 57.4	0.6	51.4	46	–	3.0	–	
EIS 0050−2933	00 50 40.5	−29 33 36.6	0.6	54.3	42	–	3.4	–	

Table 2. Cluster candidates for EIS Patch A that are found in the region where both I and V-band data are available. In addition to the information already presented in Table 2 of Paper II, here also the V-band detection significance is listed. The format of the table is the same as for Table 1.

Cluster name	α (J2000)	δ (J2000)	z	Λ_{cl}	N_R	σ_{even}	σ_{odd}	σ_V	Notes
EIS 2236−4017	22 36 18.0	−40 17 54.9	0.6	107.8	47	5.8	6.8	4.2	
EIS 2236−4026	22 36 47.6	−40 26 17.4	0.4	44.0	15	–	4.2	3.6	
EIS 2240−4021	22 40 07.8	−40 21 08.0	0.3	41.2	21	4.9	5.4	5.0	
EIS 2243−4013	22 43 01.3	−40 13 58.2	0.2	36.3	16	6.1	5.9	4.8	
EIS 2243−4010	22 43 01.9	−40 10 24.8	0.3	39.1	26	5.4	–	3.8	
EIS 2243−4025	22 43 23.8	−40 25 49.9	0.2	28.9	6	6.2	5.5	3.2	
EIS 2243−4008	22 43 47.4	−40 08 47.0	0.3	34.3	30	–	4.4	2.8	
EIS 2244−4014	22 44 01.0	−40 14 29.6	0.6	75.7	33	–	4.2	–	
EIS 2244−4019	22 44 28.4	−40 19 46.5	0.3	38.3	27	4.9	4.6	5.1	
EIS 2246−4012	22 46 30.1	−40 12 48.4	0.2	34.6	19	5.8	–	–	
EIS 2246−4012	22 46 48.5	−40 12 48.2	0.4	39.5	32	3.2	3.6	3.6	
EIS 2248−4015	22 48 54.8	−40 15 18.8	0.3	36.2	26	4.6	4.4	3.7	
EIS 2249−4016	22 49 33.9	−40 16 33.7	0.6	63.2	42	3.4	3.6	3.2	
EIS 2236−4008	22 36 46.0	−40 08 45.2	1.0	184.1	49	3.1	–	–	
EIS 2238−4010	22 38 36.0	−40 10 36.6	0.8	89.1	20	3.0	–	–	
EIS 2244−4013	22 44 59.3	−40 13 08.1	0.9	130.2	82	2.6	3.2	–	

plain the fact that they were detected only in the odd catalogs. Note that 2 of them were detected in the V catalogs. From this examination one also encounters cases where superposition of clusters at significantly different redshifts may occur, as judged from the available color information.

The cluster-finding pipeline was also used to detect cluster candidates in the available $V-$band catalogs for patches A and B. For this purpose the same radial profile as for the $I-$band data, and the same slope of the Schechter function were adopted, while the characteristic magnitude was taken from Postman et al. (1996) $M_V^* = -21.03$, corrected to the Johnson system according to the transformation given by those authors. Furthermore the limiting magnitude was chosen to fit the 80% completeness limit for the $V-$band catalogs of $V = 24.0$. Even/odd $V-$band candidate catalogs were produced, using the same peak finding criteria given above, but in contrast to the I-band procedure no selection criteria on detection significance, persistency or cluster richness (see Paper II) were imposed.

These detections were cross-identified with the I-band ones listed in Table 1, and those listed in Paper II for which $V-$band data are available (16 candidates). The latter are listed in Table 2, which reproduces part of Table 2 in Paper II, adding also the

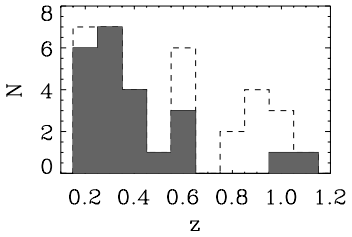

Fig. 1. The estimated redshift distribution for the 35 cluster candidates detected in regions where color information is available in patches A and B. The shaded region marks the distribution for candidates detected in both I- and V-band.

V-band information. The matching between the I- and V-band catalogs was done based on position only, using a search radius of 1 arcmin, centered on the nominal $I-$band detection. The choice of 1 arcmin was dictated by the estimated uncertainty in the position derived for the cluster candidates. It should be noted that in most cases where a match is found, the estimated redshifts agree to within $\Delta z \sim 0.1$. Only in 5 cases the discrepancy was larger. The significance of the detections in the V-band for the case of patch B cluster candidates is given in Column (9) of Table 1 and for patch A in Column (9) of Table 2. In case the candidate is detected both in the even and in the odd catalogs, the listed V-band significance is the highest of the two.

In total there are 35 candidate clusters where color information is available over a 2 square degree area. The regions where color information is available are typical regions with respect to the data quality as characterized by the seeing and limiting isophotes. The distribution of estimated redshifts for this sample is shown in Fig. 1. The median estimated redshift for the whole set presented in this figure is $z \sim 0.5$. The shaded portion of the histogram shows the distribution of estimated redshifts (as obtained from the I-band detection) for the cluster candidates also detected in V-band (combining patches A and B). Out of 19 candidates with $z \leq 0.5$, 18 ($\sim$ 95%) are also detected in V-band; for clusters at $z > 0.5$, 5 out of 16 are detected in V-band. This result is not surprising since the ability to detect clusters varies with redshift, with the redshift range of the candidates detected in V-band being smaller than that of those detected in I-band. Using the rule of thumb that the data should reach at least one magnitude fainter than m^* at the redshift of a given cluster to allow for its detection, one can translate the galaxy catalog limiting magnitudes adopted in the cluster search into limiting redshifts for cluster detection. The I-band limit of $I = 23.0$ then translates into a limiting redshift between $\simeq 1.0$ (no-evolution model) and $\simeq 1.3$ (passive evolution model). These values are in good agreement with the results presented in Paper II, and by Postman et al. (1996), where cluster detections are limited to $z \lesssim 1.1$. Using the same argument, the V-band limit of $V = 24.0$ translates into a limiting redshift between $\simeq 0.55$ (no-evolution) and $\simeq 0.7$ (passive evolution). This argument is consistent with the above findings, providing strong support for the reality of the detected candidates. Note that the two matched detections with estimated redshift $z \geq 1$ are among the cases where a significant discrepancy between redshifts estimated from the V- and I-band data is present, with the V-band estimate being significantly lower than the I-band one.

The probability of detecting a cluster also depends on its richness. Despite the small number statistics, nearby candidates not detected in V data tend to be poor, with an estimated richness close to the lower limit adopted for the inclusion of a candidate in the catalog ($\Lambda_{cl} \sim 30$). At high-redshifts, only very rich clusters, probably with a large fraction of ellipticals, are detected in the two passbands. There are two such cases in the above table, but note that neither would have been included as cluster candidates based on the V detection alone. Their appearance on the images strongly suggests that both are likely to be clusters at high redshifts. However, since some galaxies are seen in the V images, either their matched filter redshifts are overestimated or there are foreground concentrations leading to their detection in the V data. Only spectroscopic follow-up will be able to resolve such cases.

3.2. Color-magnitude diagrams

The availability of data in two passbands can, in principle, provide an alternative way of confirming cluster candidates and their estimated redshifts, based on the detection of the sequence of cluster early-type galaxies in a CM diagram. As described in paper III a color catalog was constructed for regions where multi-band data were available. The color catalog was built by merging of the $V-$ and $I-$band catalogs, associating objects based on their extension (see Paper III for further details). Using this color catalog a color-magnitude diagram, based on magnitudes measured within a 5.3″ aperture, was constructed for each cluster candidate. This diagram includes all galaxies within a radius of 0.5 h^{-1} Mpc (H_0 = 75 km s^{-1}/Mpc) from the nominal cluster position that are detected in both bands. Fig. 2 shows these diagrams for all cluster candidates with $z \leq 0.6$. Also indicated in the plot are the values of m_I^* and the color of a typical elliptical (no-evolution) at the estimated redshift of the cluster, as derived from the matched filter. At low redshift, the sequence of early-type galaxies is clearly visible, but at $z \gtrsim 0.5$ the evidence for a CM relation is, in most cases, less compelling. In no cases with $z \geq 0.7$ a CM sequence was visible, because of the relatively shallow V-band data.

Considering the combined patch A and B sample, one finds that out of 35 clusters in the region of overlap of the V- and I-band images, there are 11 with evidence for a CM relation, with redshifts extending out to $z \lesssim 0.6$. Furthermore, the redshift estimates based on color and the matched filter seem to agree, in most cases, within 0.1. In addition there are 6 cases in that redshift range where there is a weaker suggestion of a color sequence.

Comparison between the cases detected in both I and V and the cases where a color sequence is found shows that in most cases (16 out of 17) where the CM-diagram supports the detection, also the candidate is detected in both bands. There are 4 cases where a detection is found in both V and I-band and no color sequence is seen. All of these cases have signif-

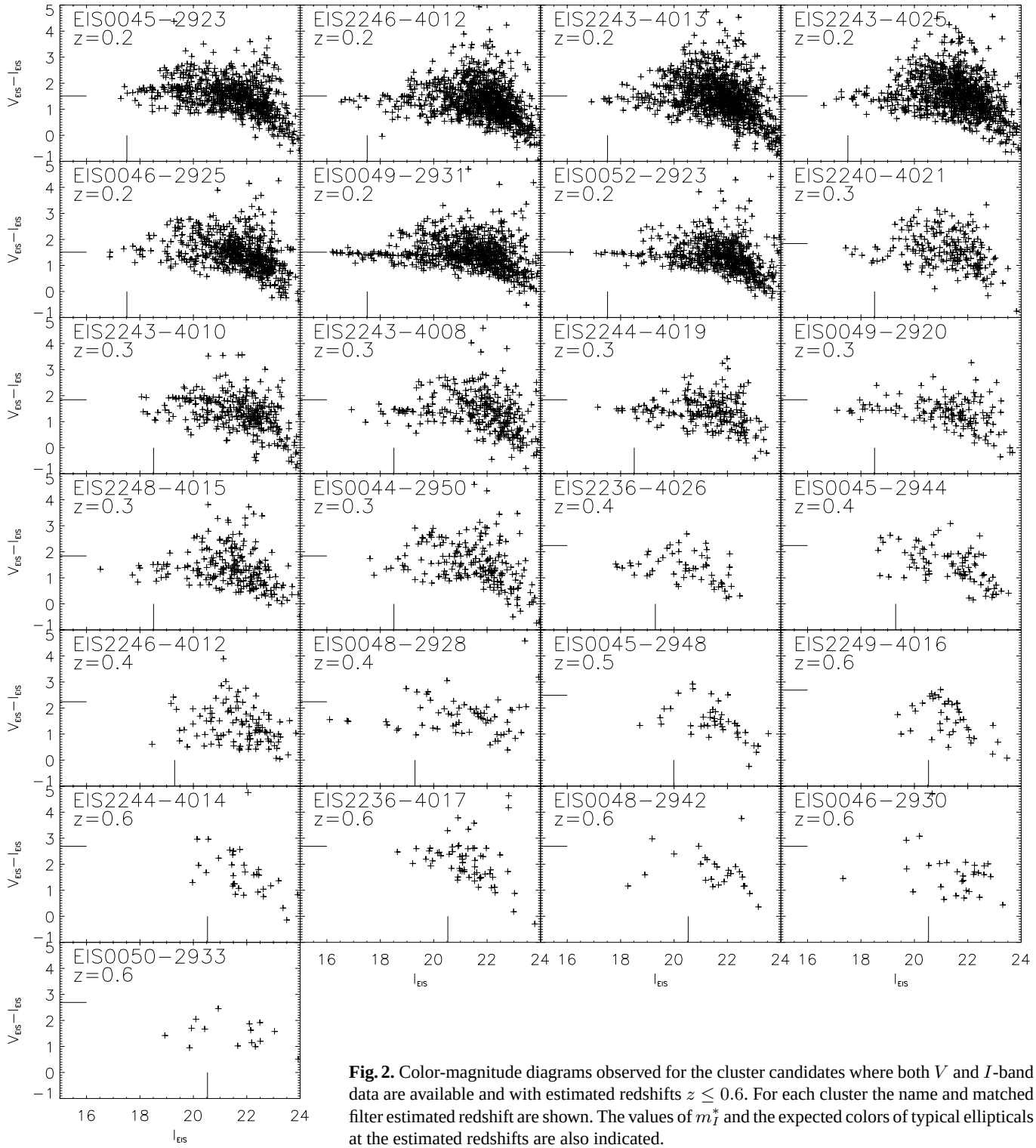

Fig. 2. Color-magnitude diagrams observed for the cluster candidates where both V and I-band data are available and with estimated redshifts $z \leq 0.6$. For each cluster the name and matched filter estimated redshift are shown. The values of m_I^* and the expected colors of typical ellipticals at the estimated redshifts are also indicated.

icances below 4, and two of them correspond to the matched detections with $z \geq 1$ shown in Fig. 1. In one case evidence for a color sequence is found but there is no detection in the V-band. Altogether this shows that the V- and I-band data provide a consistent picture, giving further support to the reality of the detections based on I-band data only.

4. Conclusions

In this paper 19 additional cluster candidates detected in EIS patch B have been presented. Cluster candidates have also been identified using the V-band galaxy catalogs available for patches A and B. The analysis of the cross-identification of the

Table 3. Summary of the cross-identification rates.

	Patch B	Patch A
I-detections	100%	100%
V-detections $z \leq 0.5$	100%	90%
V-detections $z > 0.5$	20%	30%
CM detections $z \leq 0.5$	78%	80%
CM detections $z > 0.5$	0%	0%

V- and I-band detections, as summarized in Table 3, leads to the following general conclusions:

1. About 95% of the cluster candidates with $z \leq 0.5$ and about 30% with $z > 0.5$, primarily rich clusters, are confirmed using the V-band data. This result provides confidence about the reality of the cluster candidates detected in the areas where only I-band data are available.
2. About 80% of the low redshift ($z \leq 0.5$) candidates show a suggestion of the CM relation expected for early-type galaxies in clusters. This detection serves as an independent confirmation of the candidate clusters. It also provides an independent redshift estimate, which is in general consistent with the estimates from the matched filter method.
3. The well-defined CM relations provide the possibility of selecting individual galaxies for follow-up spectroscopy to measure more accurate redshifts and velocity dispersions.

Unfortunately, the $V-$band data are not deep enough to use the CM relation to gain leverage for candidates at $z \gtrsim 0.5$. For future surveys using wide-field cameras, such as the Pilot Survey (Renzini 1998) to be conducted at the ESO 2.2m telescope, the option of doing significantly deeper $V-$band observations should therefore be considered.

Acknowledgements. The data presented here were taken at the New Technology Telescope at the La Silla Observatory under the program IDs 59.A-9005(A) and 60.A-9005(A). We thank all the people directly or indirectly involved in the ESO Imaging Survey effort. In particular, all the members of the EIS Working Group for the innumerable suggestions and constructive criticisms, the ESO Archive Group and ST-ECF for their support. Our special thanks to A. Renzini, VLT Programme Scientist, for his scientific input, support and dedication in making this project a success. Finally, we would like to thank ESO's Director General Riccardo Giacconi for making this effort possible.

References

Abell G.O., Corwin H.G. Jr., Olowin R.P., 1989, ApJS 70, 1
Nonino M., et al., 1998, A&A, in press, astro-ph/9803336 (Paper I)
Olsen L.F., et al., 1998, A&A, in press, astro-ph/9803338 (Paper II)
Postman M., Lubin L.M., Gunn J.E., et al., 1996, AJ 111, 615
Prandoni I., et al., 1998, A&A, in press, astro-ph/9807153 (Paper III)
Renzini A., 1998, Messenger 91, 54
Renzini A., da Costa L.N., 1997, Messenger 87, 23
Struble M.F, Rood H.J., 1987, ApJS 63, 543